مجلة الدراسات التربوية والعلمية - كلية التربية - الجامعة العراقية
العدد الخامس والعشرون - المجلد الثالث عشر - علوم الكيمياء - آب 2025 م
doi.org/10.52866/esj.2023.13.25.19

Thermodynamic study of adsorption of Brown HT dye on the surface of activated carbon prepared from Iraqi sesame husks

Muslim Amin Hassan
Tikrit University / College of Education for Pure Sciences / Department of Chemistry
Ma230040pep@st.tu.edu.iq

Ammar Ahmed Hamdoon
Mosul University / College of Education for Pure Sciences / Department of Chemistry
ammarhadoon@uomosul.edu.iq

Ahmed Saeed Othman
Tikrit University / College of Education for Pure Sciences / Department of Chemistry
Dra.dabbagh1960@gmail.com

Abstract:

To remove Brown HT dye from water, an activated carbon model was prepared from a plant source resulting from the waste of Al-Rashi factories Mosul, which was represented by Iraqi sesame husks that are produced in large quantities from these factories. It was found that one ton produces a percentage of (200-250 kg) and is not utilized due to the primitive method in the process of separating the husks.

The peels were burned after washing to the point of charring and treated with potassium hydroxide in a ratio of (1:1) at a temperature of 600 ± 50 °c for three hours. Then the resulting carbon material was taken and purified from the base by several processes, and also sublimation with 0.05 hydrochloric acid for two hours, then the medium was neutralized, and the carbon was dried and crushed. Its effectiveness was determined by measuring its ability to adsorb iodine from its aqueous solution, which is known as the iodine number, which is a rapid measure of the internal surface area. In addition, the thermodynamic functions' values for Brown HT dye adsorption were calculated.

This research included determining the optimum conditions for the adsorption process, by studying the factors affecting the adsorption efficiency, which showed that the ideal weight of the prepared activated carbon is (0.25 g) at a concentration of (7×10^{-5} M) and that the reaction equilibrium time is (50 minutes).

The experimental data were applied to the Langmuir, Freundlich, and Temkin models at different temperatures to use them in calculating the thermodynamic functions. The results of the study (through the values of ΔH, ΔS^o, ΔG^o) showed that the adsorption system is of the physical endothermic type, that the adsorption process occurs spontaneously, and that the adsorption system became more random due to the ionization of the dye, which is a salt of sodium ions.

Keywords: Activated carbon, sesame husks, Brown HT dye, thermodynamic functions.

مسلم امين حسن [1]
جامعة / كلية التربية للعلوم الصرفة/ قسم الكيمياء
Ma230040pep@st.tu.edu.iq

عمار احمد حمدون [2]
جامعة الموصل / كلية التربية للعلوم الصرفة / قسم الكيمياء
ammarhadoon@uomosul.edu.iq

احمد سعيد عثمان [3]
جامعة تكريت / كلية التربية للعلوم الصرفة / قسم الكيمياء
Ma230040pep@st.tu.edu.iq

مستخلص:

لإزالة صبغة الـ Brown HT من الماء، تم تحضير نموذج كاربون منشط من مصدر نباتي ناتج من مخلفات معامل الراشي في مدينة الموصل، والتي تمثلت في قشور السمسم العراقي التي تنتج بكميات كبيرة من هذه المعامل، حيث تبين ان الطن الواحد ينتج نسبة (Kg 200-250) ولا يتم الاستفادة منها بسبب الطريقة البدائية في عملية فصل القشور.

تم حرق القشور بعد غسلها الى درجة التفحم وعومل مع مع هيدروكسيد البوتاسيوم بنسبة (1:1) عند درجة حرارة (600 50 c̊) لمدة ثلاث ساعات، بعد ذلك اخذت المادة الكاربونية الناتجة ونقيت من القاعدة بعدة عمليات، وكذلك تم التصعيد مع (0.05) حامض الهيدروكلوريك لمدة ساعتين، ومن ثم جرى معادلة الوسط، وتجفيف ثم سحق الكاربون. تم تحديد فعالية الكاربون من خلال قياسات (EDX, XRD, BET)، وكذلك قابليته على امتزاز اليود من محلوله المائي، أي ما يعرف بالرقم اليودي والذي يعتبر مقياس سريع للمساحة السطحية الداخلية، فضلا عن ذلك تم حساب قيم الدوال الثرموداينميكية لامتزاز صبغة Brown HT.

تضمن هذا البحث تحديد الظروف المثلى لعملية الامتزاز، وذلك من خلال دراسة العوامل المؤثرة على كفاءة الامتزاز، والتي أظهرت أن الوزن المثالي للكربون المنشط المحضر هو (0.25 غم) عند تركيز (7×10^{-5}M) وأن زمن توازن التفاعل هو (50 دقيقة).

تم تطبيق البيانات العملية على نماذج لانكماير، وفرندلخ، وتيمكين، وعند درجات حرارة مختلفة؛ لغرض استخدامها في حساب الدوال الديناميكية الحرارية، وقد أظهرت نتائج الدراسة (من خلال قيم $\Delta G\Delta$, ΔS^o, ^oH) أن نظام الامتزاز هو من النوع الفيزيائي الماص للحرارة، وأن عملية الامتزاز تحدث بشكل تلقائي، وأن نظام الامتزاز أصبح أكثر عشوائية؛ نتيجة لتأين الصبغة والتي هي أملاح لأيونات الصوديوم.

الكلمات المفتاحية: الكربون المنشط، قشور السمسم، صبغة Brown HT، الدوال الثرموداينميكية.

Introduction:

Water pollution with dyes is considered one of the most dangerous types of industrial pollution, which is mainly caused by the discharge of industrial wastewater from textile factories. Industrial dyes contain complex chemicals that are difficult to break down naturally, which leads to their accumulation in surface and groundwater, causing negative effects on the environment and public health, as they hinder the process of photosynthesis in aquatic plants by preventing the penetration of light, and affect the oxygen balance in the ecosystem. Some dyes also contain toxic and carcinogenic compounds, which increase their risks to human health and living organisms (Uddin, F, 2021).

Activated carbon is a carbonized material with high porosity and high surface area, and has many applications in the field of environment and industry to remove, recover, separate and modify various compounds in the liquid and gaseous phases (Heidarinejad et al, 2020).

The use of carbon dates back to (3750) BC, to reduce copper (Cu), zinc (Zn) and tin (Sn) ores in the bronze industry by the Egyptians and Sumerians. In (157) AD, plant and animal carbonates were used to treat a wide range of diseases (Pandey, R. et al, 2023).

(Al-Hyali, 2013) studied the adsorption of diazolidinyl dyes on commercial activated carbon. The results showed that the Langmuir model and Freundlich model were applicable to adsorption. From a kinetic perspective, it was found that the adsorption process followed the pseudo-second-order reaction model.

(Liu et al, 2018) also adsorbed the azo dye Direct Red 23 on the surface of tourmaline powder. The study showed that the adsorption efficiency increased at low pH, and the adsorption followed the Langmuir and Freundlich models, indicating that there were heterogeneous adsorption sites on the tourmaline surface. The adsorption was of the endothermic type. (Tunali et al, 2021) were able to prepare a magnetic adsorbent based on magnetic montmorillonite (MagMt) using the co-precipitation method, which facilitates the separation process after adsorption.

The results showed that (MagMt) achieved an adsorption efficiency of

(98.60%) for Bismark Brown-Y (BB-Y) dye at pH 4 and using 40 mg of adsorbent, within 10 minutes. The adsorption process was subjected to the pseudo-second-order model and the Langmuir model.

Also, (Hanoody et al, 2024) were able to adsorb two types of azo dyes on activated carbon prepared from fallen eucalyptus leaves in the forests of Mosul city in northern Iraq, and the Freundlich model was the most suitable for the practical adsorption data, and the adsorption was physical.

Brown HT Dye:

Chocolate Brown HT E155 is an organic food azo dye, reddish brown in color, odorless, given the symbol (EEC.NO.E-155), the state of the substance is solid in the form of fine powder or granules, its density is (0.7), its solubility is (180 mgr/liter), its hydrogen atom (pH= 4-6), its molecular color is (652.57), its molecular formula is ($C_{22}H_{18}N_4Na_2O_9S_2$), its chemical name is (Abbas, 2000):

Disodium 4,4’-[(2,4-dihydroxy-5-hydroxy-methylphenyl)azo] bis(5-hydroxy-6-methyl-3-sulfonato-2,7-naphthalene disulfonate)

Its structural formula is:

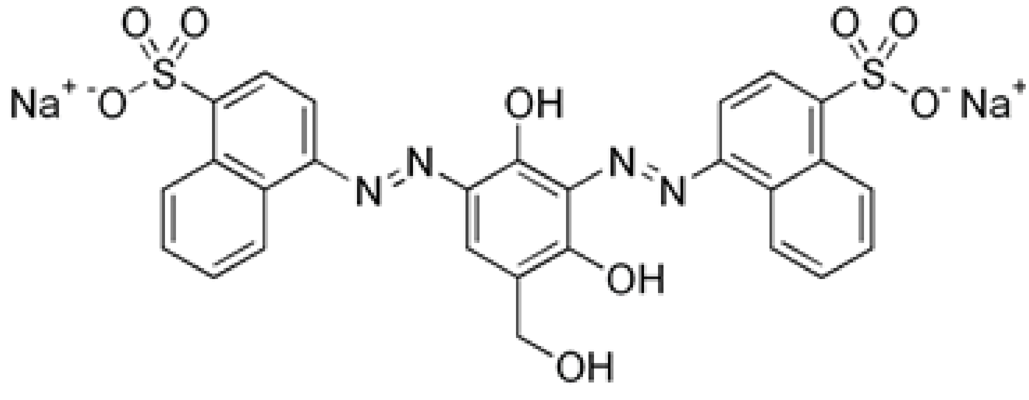

Figure (1) The structural formula of Brown HT dye

Practical part:

First: Wash the peels and burn them until charred.

Second: Preparation of activated carbon:

The material resulting from the (first) step was taken and treated with potassium hydroxide in a ratio of (1:1) at a temperature of (600 ± 50 ℃) for three hours. Then, the carbon material was cooled and washed with distilled water several times until neutralization, then treated with a 5% hydrochloric acid solution by thermal sublimation for two hours, then the carbon material was cooled and filtered and then washed with distilled water several times until neutralization, then dried and stored with a particle size of 150 micrometers, making it ready to measure its effectiveness.

Third: Determining the effectiveness of activated carbon:

A- Adsorption of iodine from its aqueous solution:

One gram of the prepared activated carbon was taken and placed in a conical flask with a capacity of (250 ml) and (100 ml) of iodine solution with a concentration of (0.1 normal) was added to it and the mixture was shaken for half an hour, then the dye solution was separated by filtration, taking into account ignoring (20 ml) of the solution at the beginning of the filtration to avoid the effect of the adsorption of the filter paper on the dye solution as well as the calibration process.

To complete the measurement, (50 ml) of iodine solution was taken and calibrated with aqueous sodium thiosulfate solution with a concentration of (0.1 N) using starch as a reagent medium. The volume of thiosulfate used to calculate the iodide absorbed by the prepared activated carbon was calculated according to the relationship (İbraheem, S et al, 2024):

X= A-[2.2B × ml of Thiosulfate Used].......(1)

A= N1 ×12693 ....(2)

B= N2 ×126.93 ....(3)

X: weight of iodine adsorbed in mg by the activated carbon, N1,N2: standard of iodine solution and standard of sodium thiosulfate respectively (0.1 N).

The iodine number is calculated through the equation:

$$I.N. = \frac{X}{MD} \;........(4)$$

Where X: weight of carbon used, D: correction factor.

B- Adsorption:

1- Making a calibration curve for Brown HT dye:

At the beginning of the study and before starting the adsorption experiments, multiple concentrations were prepared ranging between (1×10^{-5} - 9×10^{-5} M) to determine the wavelength of maximum dye absorption; to be used in measuring concentrations before and after the adsorption process. A relationship was drawn between the absorption and concentration to obtain a main equation based on the Beer-Lambert law (Aleboyeh et al, 2005):

$$A = \varepsilon LC \ldots\ldots\ldots\ldots(5)$$

(A) represents the dye absorbance, (Ɛ) the molar absorption coefficient ($L.mol^{-1}.cm^{-1}$), L the optical path length of visible light (L = 1 cm), and C the molar concentration ($mol.L^{-1}$).

2- Effect of the amount of adsorbent:

The effect of the amount of adsorbent on the adsorption efficiency was studied using a dye solution with a concentration of ($7x10^{-5}M$) with changing the amount of adsorbent in a range between (0.05 - 0.25 g) and at a temperature of (25 ℃) and a volume of (10 ml).

3- Determining the equilibrium time:

To determine the time required for equilibrium, the dye solution was prepared at the same concentration above, and an amount of (0.15 g) of activated carbon was taken, and a volume of (10 ml), with the absorbance measured at different times ranging between (5, 10, 20, 30, 40, 50, 60, 70) minutes.

4- Calculating thermodynamic functions:

The values of adsorption enthalpy (ΔH) can be calculated by calculating the value of the equilibrium constant at different temperatures (Al-Hyali et al, 2016):

$$\ln K = \text{Const.} - \frac{\Delta H}{RT} \ldots\ldots\ldots(6)$$

The value of the equilibrium constant can be calculated using the equation:

$$K = \frac{C_{ad}}{C_e} \ldots\ldots\ldots(7)$$

The value of (ΔH) was calculated by plotting a relationship between (ln K) versus (1/T); to give a straight line with a slope equal to (-ΔH/R), and (R) represents the gas constant (8.314 $J.mol^{-1}.k^{-1}$), while the values of (ΔG°) and (ΔS°) were calculated based on the following equations (Ali Mohsin et al, 2022):

$$\Delta G^{\circ} = -RT\ln K \ldots\ldots(8)$$

$$\Delta S^{\circ} = \frac{(\Delta H^{\circ} - \Delta G^{\circ})}{T} \ldots\ldots\ldots(9)$$

5- Application of adsorption isotherms:

First: Langmuir isotherm:

When drawing a relationship between C_e/q_e versus C_e, it gives a slope $(1/q_{max})$ and a section $(1/bq_{max})$ at different temperatures:

$$\frac{C_e}{q_e} = \frac{1}{bQ_{max}} + \frac{C_e}{Q_{max}} \ldots\ldots\ldots(10)$$

C_e represents the concentration of the unadsorbed material (mg/l), q_e represents the amount of adsorbed material (mg/g), while b represents the Langmuir isotherm constant ($L.mg^{-1}$) related to the adsorption energy, and Q_{max} represents the maximum adsorption capacity (Mikolajczyk et al, 2024).

Second: Freundlich isotherm:

Freundlich equation can be expressed by the following relationship:

$$\log q_e = \log K + \frac{1}{n}\log C_e \ldots\ldots\ldots(11)$$

The values of K and n represent Freundlich constants, and their values depend on the nature of the adsorbent, the adsorbent surface, and the temperature, while the value of q_e represents the amount of adsorbent (mg of adsorbent/per gram of adsorbent), and C_e represents the concentration of the unadsorbed substance at equilibrium ($mg.liter^{-1}$). When drawing a relationship between log q_e versus log C_e, a straight line with a slope of (1/n) is given, which represents a measure of the intensity of adsorption, and a line segment of log K, which is a function of the adsorption capacity (Yaffar et al, 2025).

Third: Temkin isotherm:

The linear form of Temkin's equation is as follows:

$$q_e = B_T \ln K_T + B_T \ln C_e \ldots\ldots\ldots(12)$$

Where B_T = RT/b, T is the absolute temperature (K), R is the gas constant (8.314 J.mol/K), b is a constant related to the heat of adsorption (J/mol), and (Liter / mg) K_T is the equilibrium bonding constant, which indicates the maximum bonding energy, and B_T is a constant related to the differential surface capacity for dye adsorption per unit bonding energy. By drawing the relationship between q_e versus $\ln C_e$, the values of the constants B_T and K_T can be found from the slope and intercept values, respectively (Singh, M. et al,2024).

Results and discussion:

To know the quality and efficiency of the prepared activated carbon, several measurements were conducted, including (EDX, XRD, and BET). The results are presented in Figure (2) and Table (1):

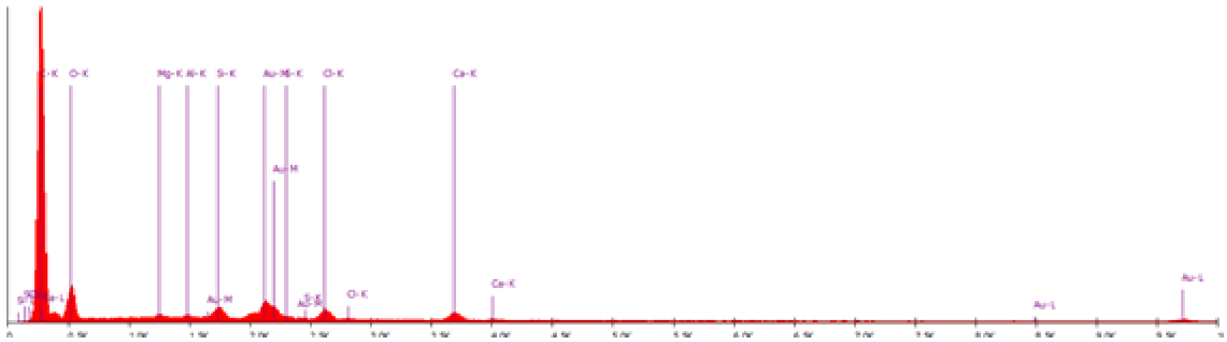

Figure (2) EDX measurement of carbon

Table (1)

Element ratios on the surface of the prepared activated carbon

Element	Atomic (%)	Weight (%)
Carbon	90.32	86.60
Oxygen	8.88	11.35
Chlorine	0.24	0.68
Silicon	0.23	0.53
Calcium	0.14	0.44
Magnesium	0.09	0.18
Sulphur	0.05	0.12
Aluminum	0.05	0.11

The EDX measurement indicated that the percentage of carbon was (90.32%), followed by oxygen at (8.88%), with very small percentages of other elements that may have appeared during preparation or were present in the original material.

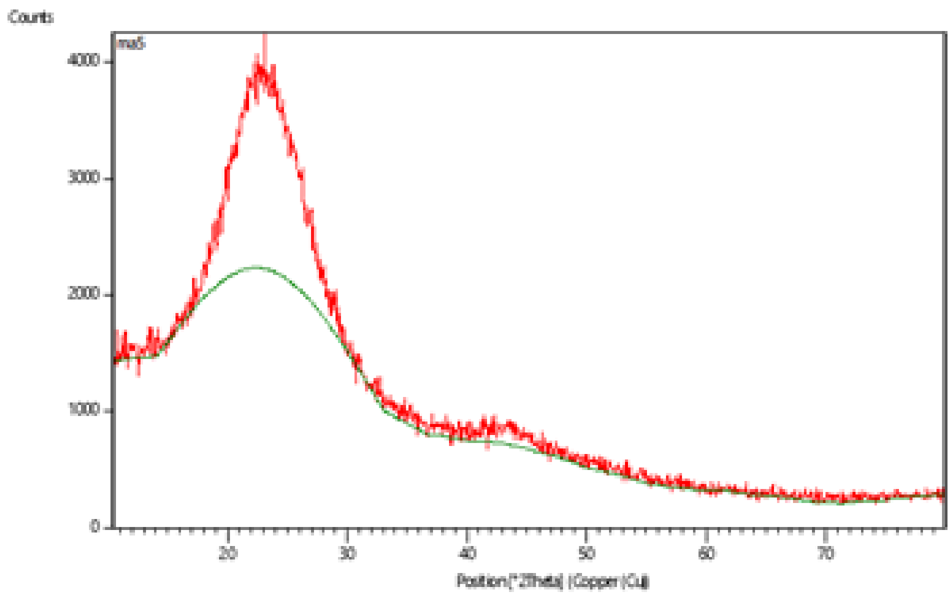

Figure (3) XRD measurement of carbon

X-ray diffraction (XRD) measurements indicated that the prepared sample was non-crystalline, as evidenced by the wide 2-theta band, which ranged from 20 to 30 (Wibawa et al., 2020). The results of adsorption measurements using the BET method showed that the prepared activated carbon had a large surface area, small pore volume, and small average pore diameter, as shown in the following table (Bicil & Dogan, 2021).

Table (2) BET measurement

Mesurement	Analysis Data
Surface area	(m^2/g) 493.43
Pore volume	(cm^3/g) 0.3147
Average pore dimeter	(nm) 2.5514

The process of preparing activated carbon using hydroxides is one of the most important preparation methods, and is considered the most important, as it is a process of carbonization and activation at the same time. The hydroxide ions present in potassium hydroxide work to withdraw hydrogen from the raw material in the form of H_2O, leaving the positive ion to control the size and type of pores formed in the activated carbon. It was found that the radius of the positive ion controls the size, type, and efficiency of the pores formed in activated carbon (Mendes et al, 2021).

When measuring the effectiveness

of carbon in absorbing iodine from its aqueous solution, it gave an iodine number of (934.2).

1- Making a calibration curve and finding the wavelength of maximum absorption:

After measuring the dye absorption at concentrations ($1x10^{-5}$ – $8x10^{-5}$ M), it was found that the dye obeys the Beer-Lambert law and obtained a high correlation coefficient:

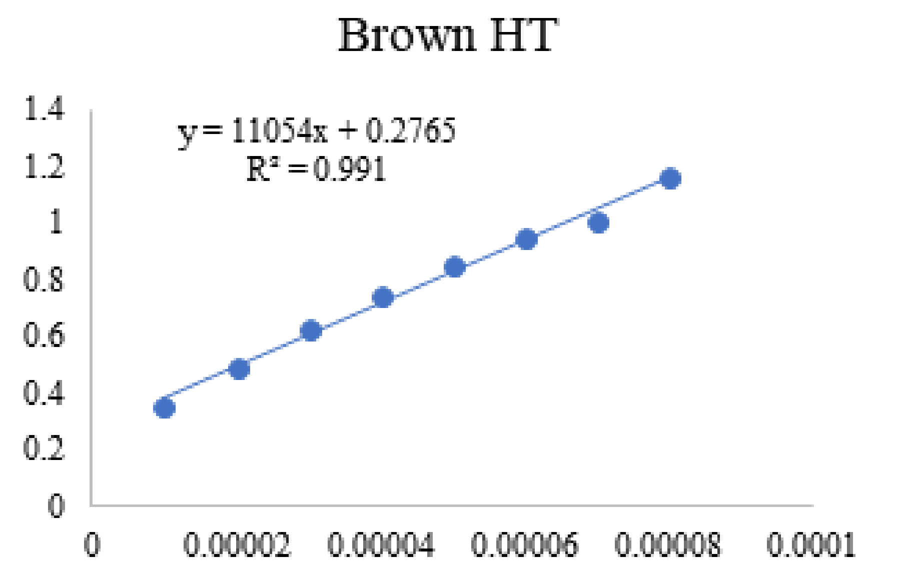

Figure (4) Calibration curve for Brown HT dye

2- Effect of the amount of adsorbent: After studying the effect of the amount of adsorbent, the following results were obtained:

Table (3) Effect of the amount of activated carbon on the adsorption efficiency at a temperature of (25c°) and a concentration of ($7x10^{-5}$ M)

Dye	C (g)	Abs	C_e (mg / l)	q_e (mg/g)	Efficiency %
Brown HT	0.05	0.592	28.023	3.531	38.65
	0.10	0.346	15.026	3.065	67.11
	0.15	0.200	7.312	2.558	83.99
	0.20	0.116	2.874	2.140	93.71
	0.25	0.066	0.232	1.818	99.49

The adsorption efficiency values showed that the preferred weight for activated carbon adsorption is (0.25 g), which means that increasing the amount of adsorbent leads to an increase in the number of sites eligible for adsorption, and this increase increases the efficiency of the adsorbent in removing the dye from the aqueous solution (Zheng et al, 2024). (0.15 g) of activated carbon was chosen to conduct subsequent studies within this study; because; large quantities lead to complete removal, which makes the study difficult.

3- Determine the equilibrium time:

By measuring the absorbance at different times using (10 ml) of the dye solution and concentration (7×10^{-5} M) at a temperature of (25 ℃), the results were obtained as shown in Table (4):

Table (4)
Effect of reaction time on adsorption efficiency

Dye	t (min)	Abs	C_e (mg / l)	q_e (mg/g)	Efficiency %
Brown HT	5	0.451	20.574	1.674	54.96
	10	0.303	12.754	2.195	72.08
	20	0.286	11.856	2.255	74.04
	30	0.263	10.641	2.336	76.70
	40	0.235	9.162	2.435	79.94
	50	0.212	7.946	2.516	82.60
	60	0.320	13.652	2.135	70.11
	70	0.323	13.811	2.125	69.77

We noticed from Table (4) that the equilibrium time was in minute (50), to be the time that will be adopted in subsequent studies, and the equilibrium time in adsorption reactions is the period of time that the adsorbent (solid or surface) takes to reach an equilibrium state with the adsorbent (molecules in the gas or liquid phase). This depends largely on the stages of the molecules' transfer from the solution to the adsorbent surface. The process is fast at the beginning due to the availability of a large number of empty sites on the adsorbent surface (external diffusion), then the number of these sites begins to decrease, which creates a kind of competition between the dye molecules for the available sites, so the speed of the molecules' transfer decreases little by little until they reach the equilibrium state where the adsorption and separation rates are equal, and all of this process is controlled by many factors, including: the size of the molecules and their polarity, as well as the surface area of the carbon and the nature of the surface in addition to the presence of effective functional groups and the degree of freedom and movement (Ho Y. S. & McKay G., 1999).

4- Calculating thermodynamic functions:

The value of (ΔH) was calculated by plotting a relationship between (ln K) versus (1/T) at different concentrations; to give a straight line with a slope equal to (-ΔH/R), where (R) represents the gas constant (8.314 $J.mol^{-1}.k^{-1}$) of the equation, while the values of (ΔG^{o}) and (ΔS^{o}) were calculated based on equations (8,9):

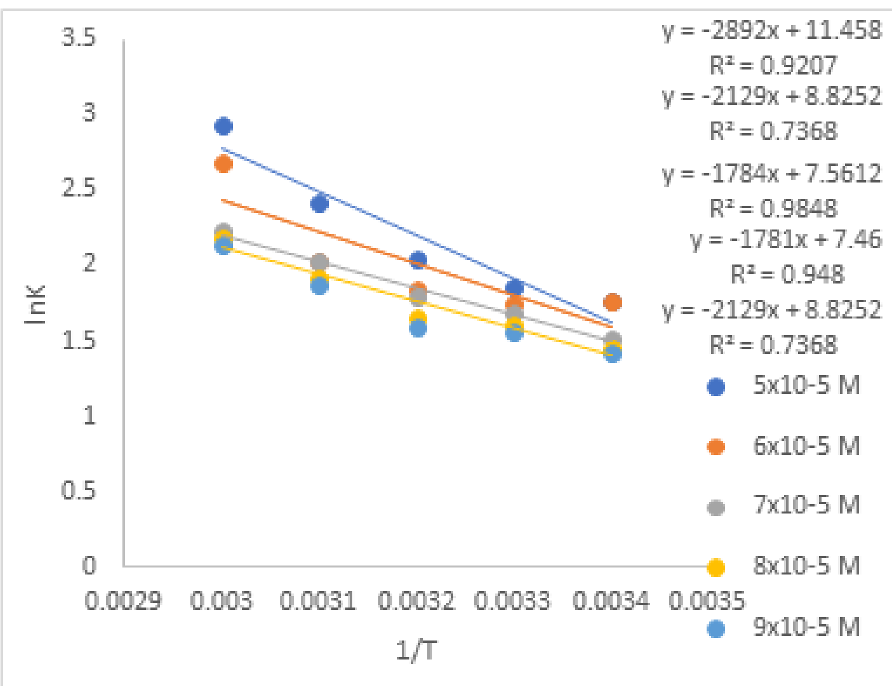

Figure (5) The relationship between lnK versus 1/T to calculate the values of adsorption enthalpy

Table (5) Values of equilibrium constants and thermodynamic functions at different concentrations and different temperatures

Daye	Conc. (M)	T (K)	K	ΔH ($kJ.mol^{-1}$)	ΔS° ($J.mol^{-1}.K^{-1}$)	ΔG° ($kJ.mol^{-1}$)
Brown	5×10^{-5}	288	5.832	24.044	98.146	-4.222
		298	6.405		96.124	-4.601
		308	7.771		95.110	-5.250
		318	11.252		95.736	-6.400
		328	18.667		97.637	-7.981
	6×10^{-5}	288	5.832	17.701	76.122	-4.222
		298	5.712		73.886	-4.317
		308	6.310		72.786	-4.717
		318	7.611		72.538	-5.366
		328	14.637		76.277	-7.318
	7×10^{-5}	288	4.564	14.832	64.122	-3.635
		298	5.385		63.768	-4.171
		308	6.006		63.062	-4.591
		318	7.611		63.516	-5.366
		328	9.367		63.820	-6.101
	8×10^{-5}	288	4.245	14.807	63.434	-3.462
		298	4.974		63.027	-3.975
		308	5.238		61.841	-4.240
		318	6.817		62.522	-5.075
		328	8.839		63.262	-5.943
	9×10^{-5}	288	4.160	14.466	62.080	-3.413
		298	4.748		61.493	-3.859
		308	4.932		60.234	-4.086
		318	6.541		61.104	-4.965
		328	8.468		61.866	-5.826

It was noted from the results listed in Table (5) that the values of the equilibrium constant (K) increase with increasing temperature and at a constant concentration, and that they decrease with increasing initial concentration, and the adsorption capacity also increases with increasing temperature, and that the positive sign of the adsorption heat values (ΔH) indicates that the nature of the association is endothermic between the dye molecules and the surface of the activated carbon, and that the results show that the values of (ΔH) are less than (40 $kj.mol^{-1}$), which proves that the adsorption is physical (Guo & Wang, 2021) and that the positive values of (ΔS°) indicate an increase in the randomness of the studied system (Ortiz et al, 2023). This may be due to the nature of the dye used, which is sodium salts that ionize in the aqueous solution, releasing sodium ions that cause an increase in the randomness of the system.

Negative values of (ΔG°) indicate that the adsorption process is spontaneous (Loutfi et al,3023), and that the spontaneity of the reaction increases with increasing temperature, due to the reaction being endothermic.

5-Application of adsorption isotherms:

First - Langmuir isotherm:

This model was applied to the experimental adsorption data by plotting a relationship between C_e/q_e versus C_e, which gives a slope ($1/Q_{max}$) and an intercept ($1/bQ_{max}$) of Eq. (10), at different temperatures (Mehr et al, 2019):

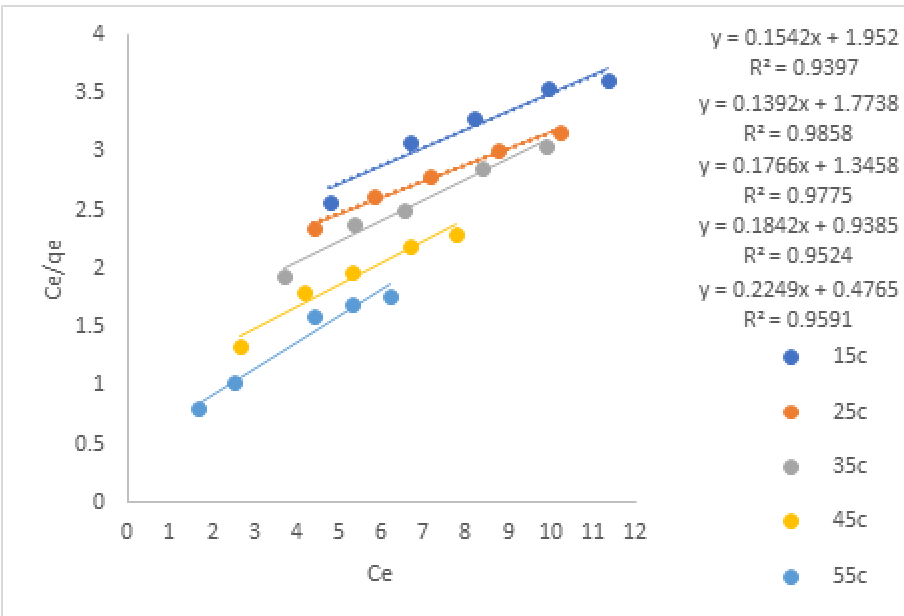

Figure (6) The relationship between C_e/q_e versus C_e for the Langmuir isotherm

Table (6) Values of the Langmuir constants and correlation coefficients obtained from the Langmuir isotherm:

T (K)	b (L/mg)	Q_{max} (mg/g)	R
288	0.079	6.485	0.9693
298	0.078	7.183	0.9928
308	0.131	5.663	0.9886
318	0.196	5.429	0.9759
328	0.472	4.446	0.9793

From Table (6), we note that the correlation coefficient is good, which indicates the possibility of applying the model to the adsorption process. We also noted an increase in the value of the constant (b) and a decrease in the value of (Q_{max}) with increasing temperature, thus consistent with the absorbent nature of adsorption (Latour, 2015).

Second: Freundlich isotherm:

The Freundlich isotherm equation (Equation 11) was applied to the experimental data at temperatures ranging between (288-328) absolute, and Freundlich constants (K_F,n) were calculated from the slope (1/n) and the intercept (log K) resulting from drawing the relationship between log qe versus log C_e:

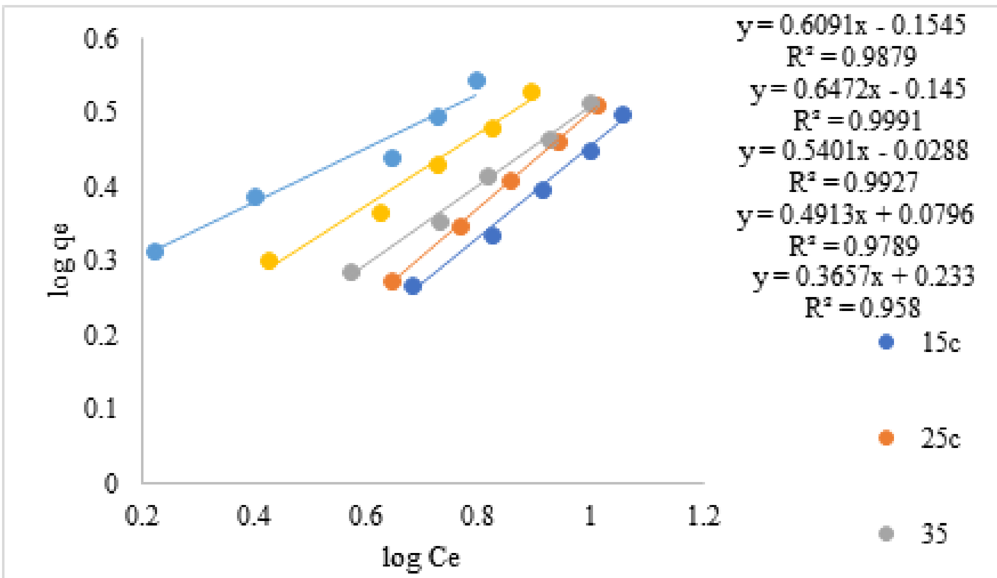

Figure (7) The relationship between log C_e versus log q_e for the Freundlich isotherm

Table (7) Values of Freundlich constants and correlation coefficients obtained when applying the Freundlich isotherm

T(K)	n	K_F	R
288	1.997	1.024	0.9986
298	1.930	1.012	0.9962
308	2.133	1.109	0.9979
318	2.102	1.128	0.9942
328	2.300	1.314	0.9834

The increase in (K_F) values indicates an increase in the ability of carbon to be adsorbed with increasing temperature, and the values of (n) between (1-10) indicate that the adsorption is of the preferred type (Javed et al, 2024).

Third: Temkin isotherm:

Using the Temkin equation (Equation 12), a relationship was drawn between (q_e) versus ($\ln C_e$) at different temperatures, where the value of (B_T) was calculated through the slope of the straight line with an intercept equal to (K_T):

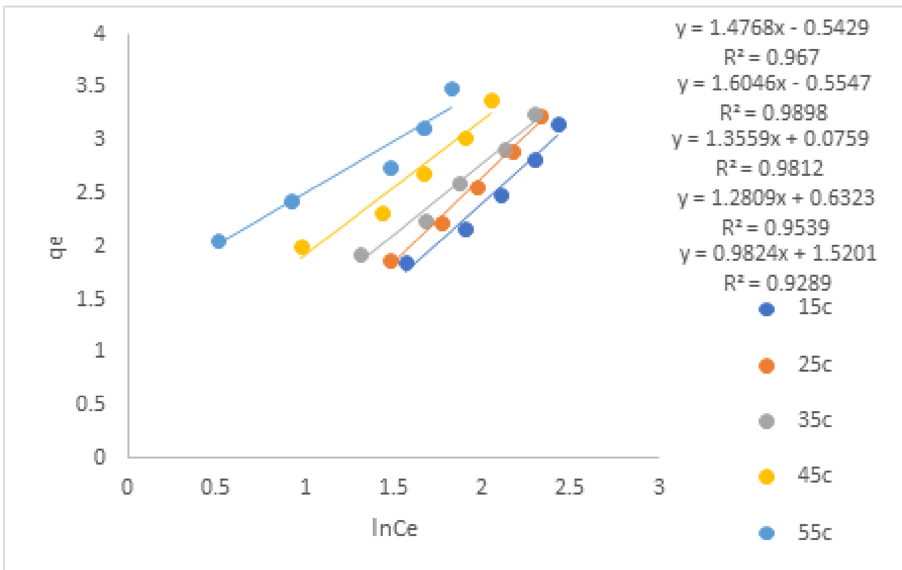

Figure (8) The relationship between q_e versus $\ln C_e$ for the Temken isotherm

Table (8) Values of the Temken constants and the correlation coefficients obtained when applying the Temken isotherm

T(K)	B_T	K_T (l/mg)	R
288	1.4768	0.5429	0.9833
298	1.6046	0.5547	0.9948
308	1.3559	0.0759	0.9905
318	1.2809	0.6323	0.9766
328	0.9824	1.5201	0.9637

The values of the correlation coefficient (R) in Table (8) indicate a good linear relationship at different temperatures, indicating the possibility of applying the Temkin isotherm to such types of systems. Also, the increase in the values of the constant (K_T) with increasing temperature is consistent with the positive sign of the heat content (Alale et al, 2025).

Conclusion:

This study aimed to prepare activated carbon from Iraqi sesame husks, an abundant agricultural waste from tahini factories, and evaluate its efficiency in removing Brown HT dye from aqueous solutions. The activated carbon was synthesized by carbonizing the husks at (600±50 ℃), followed by chemical activation using potassium hydroxide at a 1:1 ratio, and purification with hydrochloric acid. The prepared carbon was characterized using advanced techniques such as EDX, XRD, and BET, revealing a high carbon content of (90.32%) with minor impurities like oxygen and chlorine. Additionally, the carbon exhibited a large surface area (493.43 m^2/g) and small pore size (2.55 nm), enhancing its adsorption capacity.

The study demonstrated that the activated carbon achieved high efficiency in adsorbing Brown HT dye, with a removal rate of (99.49%) at an optimal dose of 0.25 g and an equilibrium time of 50 minutes at a concentration of (7×10^{-5} M). Thermodynamic analysis indicated that the adsorption process was endothermic (positive ΔH^{o} values), spontaneous (negative ΔG° values), and increased system randomness (positive ΔS^{o} values).

The adsorption data were analyzed using various isotherm models, including Langmuir, Freundlich, and Temkin. The results showed a strong fit with the Freundlich model, suggesting heterogeneous surface adsorption with a physical nature. These findings highlight the potential of sesame husk-derived activated carbon as an effective material for treating industrial dye-contaminated wastewater.

The study provides valuable insights into sustainable waste-to-resource strategies and contributes to the development of eco-friendly solutions for water purification.

REFERENCES

Abbas, Jabbar Rahim. (2000). The effect of chocolate brown dye HT E155 on some fertility parameters in male white rats. Master's thesis, College of Education, Al-Qadisiyah University.

Al-Hyali, E. A. S. (2013). Kinetic and equilibrium study of adsorption of di-azo dyes on commercial activated carbon. Pakistan Journal of Scientific & Industrial Research Series A: Physical Sciences, 56(2), 70-85.

Alale, E. M., Tulashie, S. K., Dodoo, D., Iddrisu, M., Baidoo, E. B., Addai, C. M., ... & Torgah, S. (2025). A comprehensive kinetics and thermodynamics studies of oil extraction from West African avocado: Towards sustainable development. Industrial Crops and Products, 225, 120449.

Aleboyeh, A., Moussa, Y., & Aleboyeh, H. (2005). Kinetics of oxidative decolourisation of Acid Orange 7 in water by ultraviolet radiation in the presence of hydrogen peroxide. Separation and Purification Technology, 43(2), 143-148.

Al-Hyali, E. A., Al-Khazraji, A. A., & Al-Taey, S. I. (2016). A Thermodynamic and kinetic study for adsorption of a number of dyes from their aqueous solutions on a new kind of activated carbon prepared by pomegranate (Punica granatum) peels via chemical treatment. Int J Enhanc Res Sci [Internet], 5(3), 82-116.

Ali Mohsin, A. H., Al-Niemi, H., & Mahmoud, M. (2022). Thermodynamic study for the stability of aromatic complexes formation derived from the reaction of 4-dimethyl amino benzaldehyde with diazotized dinitro aniline reagents. Egyptian Journal of Chemistry, 65(2), 421-437.

Bicil, Z., & Dogan, M. (2021). Characterization of activated carbons prepared from almond shells and their hydrogen storage properties. Energy & Fuels, 35(12), 10227-10240.

Guo, X., & Wang, J. (2021). Modeling of the fractal-like adsorption systems based on the diffusion limited aggregation model. Journal of Molecular Liquids, 324, 114692.

Hanoody, M. H., Azeez, A. A., & AL-Hyali, D. E. (2024). Adsorption Study of A Number of Di-Azo Dyes On A Nano Activated Carbon; Prepared From Stem of Eucalyptus Tree. (5), 340-359.٩.

Heidarinejad, Z., Dehghani, M. H., Heidari, M., Javedan, G., Ali, I., & Sillanpää, M. (2020). Methods for preparation and activation of activated carbon: a review. Environmental Chemistry Letters, 18, 393-415.

Ho, Y. S., & McKay, G. (1999). Pseudo-second order model for sorption processes. Process biochemistry, 34(5), 451-465.

İbraheem, S., Al-khazraji, A. A., & Al-hyali, E. A. A Statistical Study Comparing Experimental and Theoretical Yields of Activated Carbon Prepared from Pomegranate (Punica granatum) Peels via Chemical Treatment. Journal of the Turkish Chemical Society Section A: Chemistry, 11(4), 1407-1416.

Javed, T., Kausar, F., Zawar, M. D., Khalid, N., Thumma, A., Ismail, A., ... & Haider, M. N. (2024). Investigating the adsorption potential of coconut coir as an economical adsorbent for decontamination of lanthanum ion from aqueous solution. Journal of Dispersion Science and Technology, 1-12.

Latour, R. A. (2015). The Langmuir isotherm: a commonly applied but misleading approach for the analysis of protein adsorption behavior. Journal of biomedical materials research part A, 103(3), 949-958.

Liu, N., Wang, H., Weng, C. H., & Hwang, C. C. (2018). Adsorption characteristics of Direct Red 23 azo dye onto powdered tourmaline. Arabian Journal of Chemistry, 11(8), 1281-1291.

Loutfi, M., Mariouch, R., Mariouch, I., Belfaquir, M., & ElYoubi, M. S. (2023). Adsorption of methylene blue dye from aqueous solutions onto natural clay: Equilibrium and kinetic studies. Materials Today: Proceedings, 72, 3638-3643.

Mehr, M. R., Fekri, M. H., Omidali, F., Eftekhari, N., & Akbari-Adergani, B. (2019). Removal of Chromium (VI) from Wastewater by Palm Kernel Shell-based on a Green Method. Journal of Chemical Health Risks, 9(1).

Mendes, B. C., Pedroti, L. G., Vieira, C. M. F., Marvila, M., Azevedo, A. R., De Carvalho, J. M. F., & Ribeiro, J. C. L. (2021). Application of eco-friendly alternative activators in alkali-activated materials: A review. Journal of Building Engineering, 35, 102010.

Mikolajczyk, A. P., Fortela, D. L. B., Berry, J. C., Chirdon, W. M., Hernandez, R. A., Gang, D. D., & Zappi, M. E. (2024). Evaluating the suitability of linear and nonlinear regression approaches for the Langmuir adsorption model as applied toward biomass-based adsorbents: Testing residuals and assessing model validity. Langmuir, 40(39), 20428-20442.

Ortiz-Oliveros, H. B., Ouerfelli, N., Cruz-Gonzalez, D., Avila-Pérez, P., Bulgariu, L., Flaifel, M. H., & Abouzeid, F. M. (2023). Modeling of the relationship between the thermodynamic parameters ΔH° and ΔS° with temperature in the removal of Pb ions in aqueous medium: Case study. Chemical Physics Letters, 814, 140329.

Pandey, R., Wang, N., Sahu, B. B., Moharana, S., & Tiwari, S. K. (2023). Metal and Materials Engineering: Historical Prospect. In Nanoparticles Reinforced Metal Nanocomposites: Mechanical Performance and Durability (pp. 1-21). Singapore: Springer Nature Singapore.

Singh, M., Rayaz, M., & Arti, R. (2024). Isotherm and kinetic studies for sorption of Cr (VI) onto prosopis cineraria leaf powder: A comparison of linear and non-linear regression analysis. Environmental Progress & Sustainable Energy, 43(1), e14259.

Tunali Akar, S., Ozdemir, I., Sayin, F., & Akar, T. (2021). Adsorption of diazo dye from aqueous solutions by magnetic montmorillonite composite. CLEAN–Soil, Air, Water, 49(2), 2000165.

Uddin, F. (2021). Environmental hazard in textile dyeing wastewater from local textile industry. Cellulose, 28(17), 10715-10739.

Wibawa, P. J., Nur, M., Asy'ari, M., & Nur, H. (2020). SEM, XRD and

FTIR analyses of both ultrasonic and heat generated activated carbon black microstructures. Heliyon, 6(3).

Yaffar, D., Brenner, J., Walker, A. P., Craig, M. E., Vaughan, E., Marín-Spiotta, E., ... & Mayes, M. A. (2025). The Freundlich isotherm equation best represents phosphate sorption across soil orders and land use types in tropical soils of Puerto Rico. Biogeochemistry, 168(2), 1-15.

Zheng, X., Pan, C., Zheng, S., & Guo, Y. (2024). Functionalized magnetic chitosan-based adsorbent for efficient tetracycline removal: deep investigation of adsorption behaviors and mechanisms. Separation and Purification Technology, 335, 126212.